Transactions of the 15th International Conference on
Structural Mechanics in Reactor Technology (SMiRT-15)
Seoul, Korea, August 15-20, 1999

Analysis of Massive Reinforced Concrete Ring Beam of Nuclear Containment Structure due to Heat of Hydration

Raghupati Roy, U.S.P. Verma and A.S. Warudkar

Nuclear Power Corporation of India Ltd., India

ABSTRACT In massive reinforced concrete structures, the setting, and hardening of concrete is accompanied by non-linear temperature distribution caused by developing heat of hydration. This leads to development of tensile stress in concrete that may exceed tensile strength of young concrete and cause early cracking. This paper describes an effective method of predicting the temperature history in concrete due to heat of hydration. The predicted temperature history has been compared with the temperature data recorded in the ring beam of the Inner containment structure of one of the PHWR in India. The method of evaluation of stresses at the early age due to heat of hydration, creep and shrinkage and control of cracking has also been discussed in this paper.

INTRODUCTION

Heat of hydration affects concrete structure unless accounted for appropriately in the design stage. The ring beam of the inner containment structure of an Indian nuclear power plant is a prestressed reinforced concrete structure, which forms a part of the primary containment system. The ring beam is approximately 1.7-m wide and 4.5 m deep and made up of M60 (cube) grade of concrete with cement content of 475 kg/m^3. Heat of hydration of such massive structure is very important in order to avoid cracks which otherwise will increase the leakage rate. In order to minimise the effect of heat of hydration a number of measures are taken to control the effective temperature rise. Some of these measures are casting the ring beam in three pours, control of placement temperature, introduction of prestress in the old concrete below the new pour etc. The effect of heat of hydration and early shrinkage in such massive reinforced concrete structure needs a detail study from the point of view of controlling excessive cracking of the concrete at early ages.

In this paper, the methodology to estimate the temperature rise due to heat of hydration in concrete structure by solving the Fourier heat conduction equation in time domain considering the existing environmental interaction has been presented. The temperature rise in the largest pour of the ring beam has been computed using the above methodology with appropriate boundary conditions. The temperature distribution in time domain has been compared with those recorded at site.

The stress analysis of the ring beam of the inner containment has been carried out using the predicted temperature rise due to heat of hydration. The effect of autogeneous and the drying shrinkage has also been considered to explore the possibility of cracking at the early stage during construction. The early creep of concrete has been taken into account with the help of effective modulus at the early age. On the basis of detail study, it has been concluded that the model adopted in the computation of temperature profile predicts the temperature rise in the concrete structure reliably and the stresses developed in the ring beam due to heat of hydration and early shrinkage are well within permissible limits to avoid formation of large cracks.

THERMAL ANALYSIS METHODOLOGY

The Fourier heat conduction equation relating the temperature (T) in each point of the ring beam to time (t) can be written using cylindrical co-ordinate system in the following form considering the symmetry in circumferential direction

$$\rho c \;\; \delta T/\delta t = k \; (\delta^2 T/\delta r^2 + 1/r * \delta T/\delta r \;\; + \delta^2 T/\delta z^2) + q_v \qquad \text{... (1)}$$

where k = thermal conductivity (cal/°C/m/hr)
ρ = Density of the material (kg/m^3)
c = specific heat (cal/kg/° c)
q_v = rate of heat generation per unit volume (cal / hr/kg of cement)

Equation (1) is a second-order partial differential equation, which can be solved numerically using finite difference/finite element method with appropriate boundary conditions.

The boundary conditions on both the sides and on the top surface of the ring beam can be written as

$$- k * \; \delta T/\delta r. * \eta_r = q \quad \text{and}$$

$$- k * \; \delta T/\delta z. * \eta_z = q \qquad \text{... (2)}$$

where η_r and η_z are the direction cosine of the unit outward vector normal to the boundary surface and q is the heat energy transferred between the boundary and the environment.

The transfer of energy (q) between concrete and the environment takes place due to convection (q_c), thermal irradiation (q_r) and solar radiation (q_s).

The rate of energy transfer by convection due to the difference between the air temperature (T_{air}) and the concrete surface temperature (T_s), is expressed by Newton's Law

$$q_c = h_c (T_s - T_{air}) \qquad \text{... (3)}$$

Where h_c = convection heat transfer co-efficient (cal/°C/sq.m/hour)

The factor h_c depends on several factors and its correct determination is very difficult. F.A.Branco et. al. [1] has suggested the following relationship

$$h_c = h_n + h_f \qquad \text{... (4)}$$

In which h_n depends on various factors such as surface roughness. Average value of h_n for concrete surface is 6 watt/°C/sq.m/hr. h_f depends on wind speed, v(m/sec) and is approximately expressed by

$$h_f = 3.7\ v \qquad \dots (5)$$

The air temperature has been assumed to be equal to ambient temperature throughout the period of hydration for the purpose of temperature prediction whereas the actual variation of atmospheric air temperature has been considered in the final analysis after construction.

The heat energy transfer by thermal irradiation between the surface and the atmosphere can be estimated using Stefan – Boltzman Law [2] as given below:

$$q_r = h_r\,(T_s - T_{air}) \qquad \dots (6)$$

in which h_r is the irradiation heat transfer co-efficient. h_r depends on the surface temperature T_s, concrete emmissivity (ε) and the Stefan–Boltzman constant. For usual concrete surface temperature, this can be estimated as

$$h_r = \varepsilon\,[4.8 + 0.075\,(T_{air} - 5)\,] \qquad \text{where } T_{air} \text{ is in } ^{o}\text{C} \qquad \dots (7)$$

The effect of solar radiation has not been considered in the present study.

Heat of Hydration

The heat generation rate per unit volume, qv is associated to the adiabatic temperature rise. For concrete, the relationship between the adiabatic temperature rise T_a and the heat of hydration Q_h (per unit mass of cement) is given by

$$T_a = \beta/c\rho.Q_h \qquad \dots (8)$$

Where β = cement content (kg/m^3)

The heat generation rate q_v is related to the heat of hydration by the following equation

$$q_v = \beta.dQ_h/dt \qquad \dots (9)$$

and using the relationship given in equation (8), we can write

$$q_v = \rho.c.dT_a/dt \qquad \dots (10)$$

The rate and magnitude of the adiabatic temperature rise is a function of cement, and its temperature during hydration and the water-cement ratio.

The equation of adiabatic temperature rise with time can be written after Machida et. al.[3] as

$$T = K\,(\,1 - e^{-\alpha t})\quad (^{o}\text{C}) \qquad \dots (11)$$

Thus, the expression for q_v can be written as

$$q_v = (1/24).\ \rho c.\alpha.k.e^{-(\alpha t/24)} \quad (\text{cal/m}^3/\text{hr}) \qquad \dots (12)$$

Based on experience, Machida et.al proposed the value of K and α as 40.8 ^{o}C and 1.6 respectively for concrete with cement content 266 kg/m^3. In the present analysis the value of

T thus obtained have been modified proportionately for the cement content of 475 kg/m^3 and for the lower water-cement ratio in order to take into account the lower fraction of hydrated cement [4].

THERMAL ANALYSIS RESULTS AND EXPERIMENTAL STUDY

Concrete temperatures were measured in the second pour of the ring beam using resistance thermometers, which were embedded in the concrete during casting. The cross-section of the ring beam indicating the location of the resistance thermometers are shown in Fig.1 The predicted temperature history at the locations of five resistance thermometers along with the recorded temperatures are shown in Fig.2 through Fig.6

Discussion on the Results

The predicted peak temperature at the center of the pour is 67° C whereas the recorded temperature at the same location is 66° C. It may be observed from Fig-2 that the development of temperature at the center of the pour matches closely with those recorded at site and the peak temperature occurs almost at the same time. The temperature profile near the top surface also follows a similar trend as that of the measured one. However, the local difference in the predicted and the recorded temperature profile could be attributed to the presence or absence of the curing water and also other environmental parameters, which are changing with time. The bottom pour of the ring beam has been considered as a heat sink with a constant temperature. This assumption might have led to the small difference in the predicted temperature profile and the recorded temperature profile at the bottom of the pour. The temperature distribution at the side faces of the pour covered by wooden shuttering also shows similar trend as that of the recorded temperature values.

STRESS ANALYSIS METHODOLOGY

Thermal stress analysis has been carried out with the help of finite element method using axisymmetric solid elements. The method incorporates an incremental procedure in which temperature increase in each time increment is introduced in all nodes of the finite element mesh, and the associated stresses are computed.

The compressive strength of concrete varies with time. The compressive strength of concrete, f_{cj} at different time (j^{th} day) has been calculated using the following relationship [5]

$$f_{cj} = [\, j/(1.4+0.95j)]\, f_{c28} \text{ in MPa} \qquad \dots (13)$$

where $f_{c28} = 28^{th}$ day characteristic cylinder strength of concrete

The modulus of elasticity E_c (j) can be computed at early ages using the following relationship [5]

$$E_c(j) = 11000 * f_{cj}^{\ 1/3} \qquad \dots (14)$$

The creep of concrete due to thermal stresses at early ages has been accounted for using an effective modulus of elasticity, E_e obtained with a constant creep coefficient of 0.6 [3].

The strain due to the autogeneous and the drying shrinkage has been computed based on the formulation given in revised Appendix-1 of BPEL 91 applicable to high performance concrete [6]. The stress developed on account of the restrained shrinkage strain has also been added to the thermal stresses to explore the possibility of cracking at the early stage during construction.

The stresses thus computed have been compared with the tensile strength of concrete in time domain in order to explore any possibility of cracking. The tensile strength of concrete f_{tj} at any stage has been computed using the following relationship [5]

$$f_{tj} = 0.6 + 0.06\, f_{cj} \qquad \text{in MPa} \qquad \ldots (15)$$

RESULTS OF STRESS ANALYSIS

The development of hoop stress with time at the center of the pour due to heat of hydration has been shown in Fig.7. It may be observed from Fig.7 that compressive stress induced in the concrete at early ages disappears with subsequent cooling. On further cooling tensile stresses develop. The temperature stress distribution across the thickness at the mid-height of the pour at different instant has been presented in Fig.8.

The strain due to autogeneous and drying shrinkage due to the restraint provided by the older pour cause tensile stress in the concrete in the hoop direction. The net tensile stress developed in the concrete due to shrinkage and heat of hydration is always less than 2/3 f_{tj} and thus, any possibility of cracking of concrete at early ages has been ruled out.

CONCLUSION

Due to poor thermal conductivity, high temperature rise associated with non-linear temperature gradient may occur in large concrete pours due to heat of hydration. Rational computation of the temperature history in the young concrete due to heat of hydration is possible using the present formulation discussed in this paper.

On the basis of detailed stress analysis due to heat of hydration and comparison of induced tensile stresses in the young concrete with the permissible tensile stresses in the young age, it is also concluded that there exists no possibility of cracking of young concrete.

ACKNOWLEDGEMENT

The authors are grateful to Director (Engg.), Nuclear Power Corporation of India Ltd., for kindly allowing them to publish this paper.

REFERENCES

1. F.A.Branco, P.A.Mendes and E. Mirambell, " Heat of hydration effects in concrete structures," ACI Materials Journal, Vol.-89, No.-2, Mar-Apr, 1992.
2. F.A.Branco and P.A.Mendes, "Thermal actions for concrete bridge design," Journal of Structural Engineering, ASCE, Vol.-119, No.-8, Aug, 1993.
3. N. Machida and K. Uehara, "Non-linear thermal stress analysis of a massive concrete structures," Computer & Structures, Vol.-28, No.-1/2, 1987.
4. A. M. Neville, *Properties of Concrete*, ELBS publication, Third Edition, 1988.
5. BPEL-83 (English Translation), 1983, *Technical rules for the design of prestressed concrete structures using limit state method.*
6. Revised Appendix-1 of BPEL-91 (English translation), *Technical rules for the design of prestressed concrete structures using limit state method.*
7. Roy Raghupati, Verma, U.S.P. and Warudkar, A.S., "Analysis of Reactor Building Raft due to Heat of Hydration," Proc. Of 14th SMiRT, Vol.-11, August 1997.

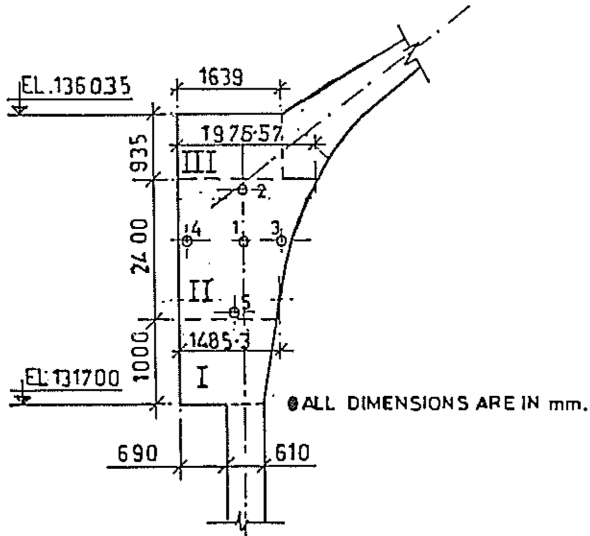

FIG.1-CROSS SECTION OF RING BEAM SHOWING THE LOCATION OF RESISTANCE THERMOMETERS IN POUR-II

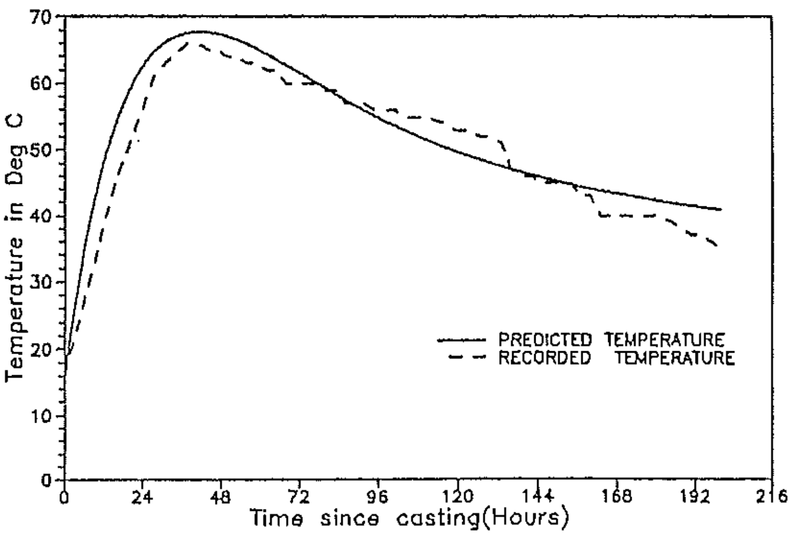

Fig.2 : TEMPERATURE DISTRIBUTION IN POUR-II OF IC RING BEAM (AT THE CENTRE OF THE POUR)

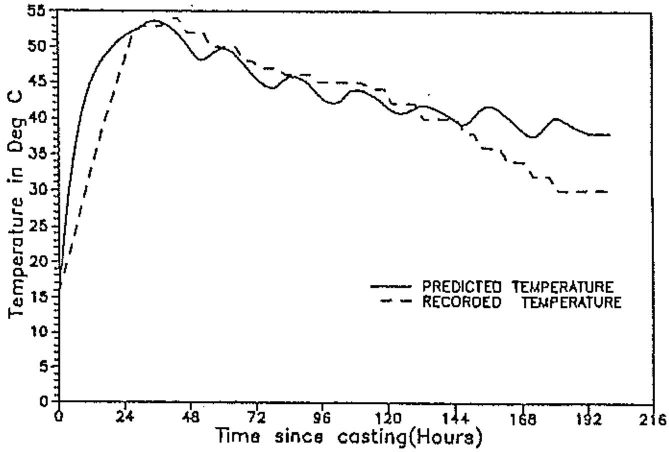

Fig.3 : TEMPERATURE DISTRIBUTION IN POUR-II OF IC RING BEAM (AT THE TOP OF THE POUR)

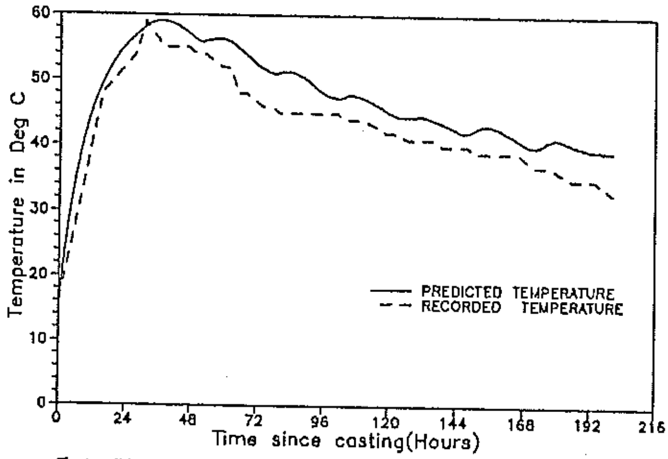

Fig.4 : TEMPERATURE DISTRIBUTION IN POUR-II OF IC RING BEAM (ON THE OUTER FACE OF THE POUR)

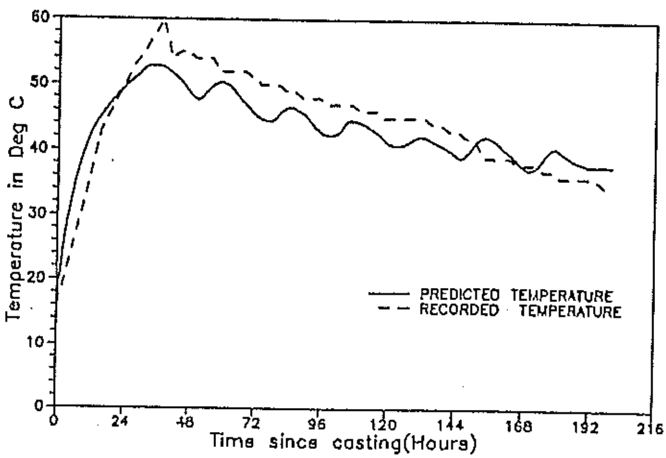

Fig.5 : TEMPERATURE DISTRIBUTION IN POUR-II OF IC RING BEAM (ON THE INNER FACE OF THE POUR)

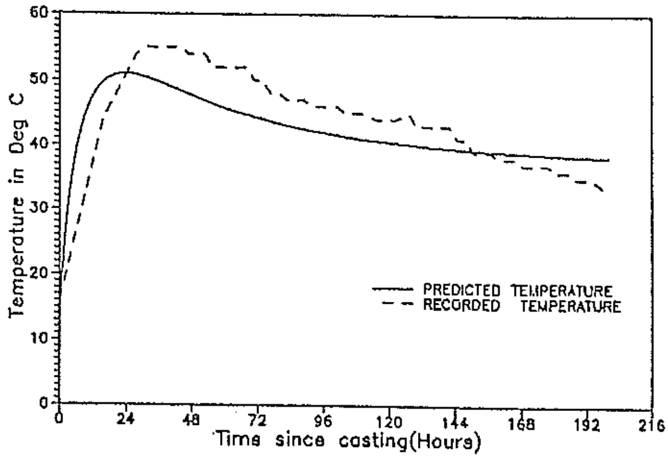

Fig.6 : TEMPERATURE DISTRIBUTION IN POUR–II OF IC RING BEAM
(AT THE BOTTOM OF THE POUR)

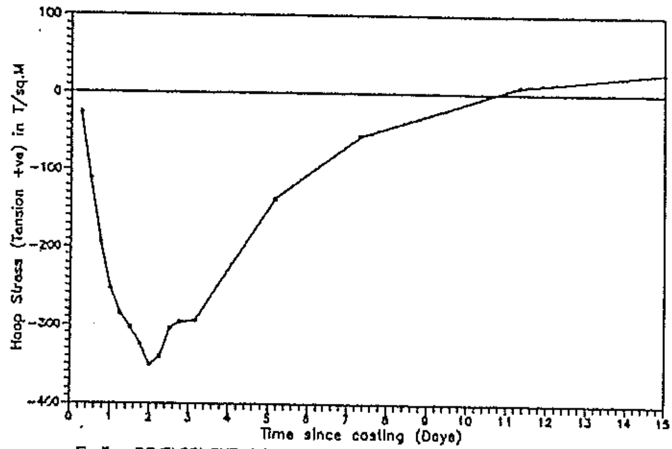

Fig.7 : DEVELOPMENT OF HOOP STRESS AT CENTRE OF THE POUR

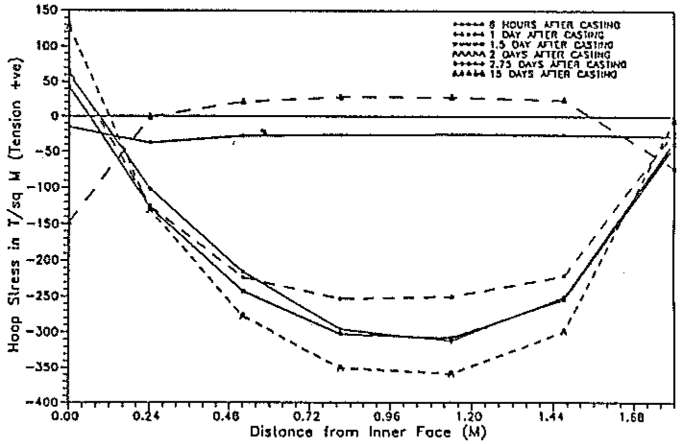

Fig.8. : HOOP STRESS DISTRIBUTION ACROSS THE THICKNESS
AT THE MID HEIGHT OF THE POUR